

# Natural Oxidation of thin Fe Films on V Buffer Layer

H. DAWCZAK-DEBICKI<sup>a,b</sup>, A. MARCZYŃSKA<sup>a</sup>, A. ROGOWSKA<sup>a,c</sup>, M. WACHOWIAK<sup>a,c</sup>,  
M. NOWICKI<sup>c</sup>, S. PACANOWSKI<sup>a</sup>, B. JABŁOŃSKI<sup>a,c</sup>, W. KOWALSKI<sup>a</sup>, J. GREMBOWSKI<sup>a</sup>,  
R. CZAJKA<sup>c</sup> AND L. SMARDZ<sup>a,\*</sup>

<sup>a</sup>Institute of Molecular Physics, Polish Academy of Sciences, M. Smoluchowskiego 17, 60-179 Poznań, Poland

<sup>b</sup>Faculty of Physics, Adam Mickiewicz University, Umultowska 85, 61-614 Poznań, Poland

<sup>c</sup>Faculty of Technical Physics, Poznań University of Technology, Piotrowo 3, 60-965 Poznań, Poland

(Received October 24, 2016; in final form September 6, 2017)

We have studied oxidation kinetics of Fe thin film under atmospheric conditions using the fact that metallic iron is a ferromagnet but ultrathin natural iron oxides are approximately nonmagnetic at room temperature. As a consequence, oxidation is associated with a loss in total Fe magnetic moment. Results show that the sample with an initial Fe thickness equal to 10 nm oxidize relatively fast (time constant  $\tau = 0.05$  day), whereby a constant amount of 2.5 nm of metal is transformed into oxides. For lower iron initial thickness ( $d_i = 4$  nm) the time constant for oxidation significantly increases reaching a value of 2 days. Furthermore, X-ray photoelectron spectroscopy studies performed after 144 days of oxidation revealed formation of hematite ( $\alpha$ -Fe<sub>2</sub>O<sub>3</sub>) thin film on the metallic rest of iron.

DOI: [10.12693/APhysPolA.132.1272](https://doi.org/10.12693/APhysPolA.132.1272)

PACS/topics: 75.70.-i, 68.55.-a

## 1. Introduction

Oxidation of metals plays an important role due to high costs of corrosion each year. On the other hand, oxidation could be also useful in preparation of thin oxide films applied for instance as catalysts, sensors, and dielectrics [1]. Binary iron oxides range from reasonable conductors (magnetite — Fe<sub>3</sub>O<sub>4</sub>) to insulators and from ferrimagnets to antiferromagnets [2, 3]. Hematite ( $\alpha$ -Fe<sub>2</sub>O<sub>3</sub>), the most stable phase in ambient conditions, is a weak ferromagnet with the corundum structure.

As is well known, all metallic thin films oxidize under atmospheric conditions. Normally this process is depth limited such that an oxide covering layer with a well-defined thickness is formed by which the underlying metal is prevented from further oxidation. In this way one can obtain a self-stabilized bilayer structure [4–6].

Iron thin films investigated here, after exposition to ambient condition actually consist of bilayer system with two magnetically active materials, namely nonoxidised metallic iron covered by natural oxide layer. The oxidized surface layer is predominantly consisted of  $\alpha$ -Fe<sub>2</sub>O<sub>3</sub>. Such a layer approximately gives no magnetic signal at room temperature compared to that measured for nonoxidised metallic Fe layer. Metallic bcc iron, on the other hand, is a well-known ferromagnet with a magnetic moment per Fe atom of about  $2.2 \mu_B$ . Formation of oxide is at the expense of the metallic Fe ferromagnet and therefore associated with a loss of the observed saturation magnetic moment. Using a sensitive vibrating sample magnetometer (VSM) we have measured the

hysteresis curves of such iron films on an absolute scale and could evaluate a quantitative measure for the amount of ferromagnetic metal being transformed into approximately nonmagnetic oxide at room temperature.

It was also reported in Ref. [4] that the polycrystalline and smooth cobalt films with an initial thickness of  $d_i > 5$  nm oxidize instantaneously, whereby a constant amount of 2.5 nm of metal is transformed into oxide. For  $d_i < 5$  nm the time constant for oxidation increases considerably and follows an approximately linear dependence with decreasing film thickness, reaching an extrapolated value of  $\tau = 190$  days for  $d_i \rightarrow 0$ . This increasing time constant lets all Co thin films with  $d_i < 2.5$  nm appear ferromagnetic for a long time due to a nonoxidised metallic rest [4].

On the other hand, smooth iron thin films may exhibit different chemical properties responsible for oxidation compared to those reported for cobalt. We have recently studied *in situ* growth of sputtered iron thin films on vanadium underlayer [7]. Results showed that the iron thin films grow on vanadium in the planar mode up to a thickness of about 5 nm. For the greater thickness we have observed a transition to island growth mode [7]. Therefore, a surprising observation that thinner ferromagnetic layers are more oxidation resistant than the thicker ones could be associated with observed transition in the growth mode [7]. The thickness dependence of the Co thin films growth on SiO<sub>2</sub> underlayer was not reported [4]. However, it is not definitively excluded that a similar transition in the Co growth on SiO<sub>2</sub> underlayer also takes place.

## 2. Experimental procedure

X-ray photoelectron spectroscopy (XPS) is an universal surface analysis technique that can be used for compositional and chemical states analysis. Since X-rays are

\*corresponding author; e-mail: [smardz@ifmpan.poznan.pl](mailto:smardz@ifmpan.poznan.pl)

used for the incident beam, the XPS technique causes very little charging of samples and thus it is useful for both electrically conductive and non-conductive materials. The information depth depends on the electron kinetic energy and emission angle [8]. For the electron energies that are normally used in XPS, the information depth are about 1–3 nm for the emission angles normal to the surface [8].

It has been shown in previous studies [1, 9–15] that the peak positions of Fe  $2p_{1/2}$  and Fe  $2p_{3/2}$  depend on the ionic states of Fe. The positions of the satellite peaks for the Fe  $2p_{1/2}$  and Fe  $2p_{3/2}$  peaks are also very sensitive to the oxidation states and these peaks have been used for qualitatively determining the ionic states of iron.

The Fe thin films with thicknesses of about 4 and 10 nm were prepared at room temperature on 2 nm V buffer layer using UHV ( $5 \times 10^{-10}$  mbar) magnetron sputtering [16–18]. As a substrate we have used Si(100) wafers with an oxidised surface to prevent a silicide formation [19–21]. Therefore we have applied a special heat treatment in UHV before deposition in order to obtain an epitaxial  $\text{SiO}_2$  surface layer [4, 22]. The Fe-layer was deposited using a DC source. For preparation of V buffer layer a RF source was used. Furthermore, we have also prepared Fe/V bilayers with the same layer thicknesses as described above but with additional 5 nm Pd capping layers. The later Fe/V bilayers were protected against oxidation by Pd and serve as reference samples in magnetic measurements.

The chemical composition and the cleanness of all layers were checked *in situ*, immediately after deposition, transferring the samples to an UHV ( $4 \times 10^{-11}$  mbar) analysis chamber equipped with XPS, Auger electron spectroscopy (AES) and ion gun etching system [23–27]. The XPS spectra were measured at room temperature using a SPECS EA 10 PLUS energy spectrometer with Al  $K_\alpha$  and Mg  $K_\alpha$  radiation of 1486.6 eV and 1253.6 eV, respectively. All emission spectra were measured immediately after the sample transfer in vacuum of  $8 \times 10^{-11}$  mbar. The  $4f_{7/2}$  peak of gold was situated at 84.0 eV and the Fermi level was located at  $E_B = 0$  eV. The measurements were conducted following routine backing procedures ( $T = 440$  K) of the analysis chamber which made possible reaching a base vacuum of  $4 \times 10^{-11}$  mbar. Details of the XPS measurements can be found in Refs. [28–30].

The morphology and roughness of the oxide layers were studied *ex situ* by atomic force microscopy (AFM). The magnetic measurements of the oxidised and reference samples were carried out using a vibrating sample magnetometer at room temperature. The total magnetic moments  $M$  were determined from the in-plane hysteresis loop measurements in magnetic fields up to 2 T.

### 3. Results and discussion

After extraction from UHV preparation chamber and exposition to ambient condition (air at room temperature) the iron thin film with an initial thickness  $d_i$  equal

to 4 nm starts to oxidise. Formation of oxide is at the expense of the metallic Fe ferromagnet (see Fig. 1) and therefore associated with a loss of the observed saturation magnetic moment. Using a sensitive VSM we have measured the hysteresis curves of such iron films on an absolute scale and could evaluate a quantitative measure for the amount of ferromagnetic metal being transformed into nonmagnetic oxide at room temperature.

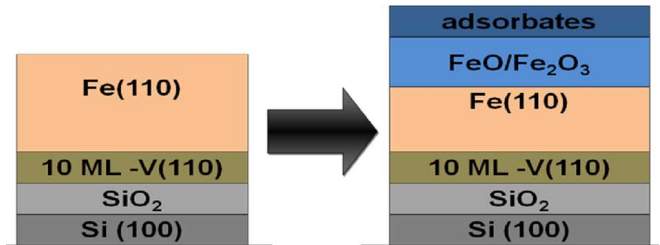


Fig. 1. Schematic description of the “as prepared” (left part) and oxidised (right part) Fe thin film at room temperature.

XPS results showed no signal from potential contamination atoms like O  $1s$  and C  $1s$ . Furthermore, in the XPS experiment we have also studied the Fe layer growth on a 1.6 nm-V underlayer. The freshly deposited 1.6 nm-V/ $d_0$ -Fe bilayer was *in situ* transferred from the preparation chamber to the analysis chamber, where the XPS Fe  $2p_{3/2}$  and V  $2p_{3/2}$  core level spectra were immediately measured in vacuum of  $8 \times 10^{-11}$  mbar. Then the bilayer was transferred back to the preparation chamber and the deposition process of the Fe overlayer was continued. The above procedure (overlayer deposition and XPS core level measurements) was repeated until the Fe  $2p_{3/2}$  and V  $2p_{3/2}$  integral intensities were saturated. Practically no trace of oxygen (or any other contaminations) adsorption or surface oxide formation was detected during the transfer operation or XPS measurements ( $\approx 10$  min). From the exponential variation of the XPS Fe  $2p$  and V  $2p$  integral intensities with increasing overlayer Fe (V) thickness up to 5 nm we conclude that the Fe and V sublayers grow homogeneously in the planar mode. Details of the growth studies could be found in Ref. [7]. We have previously observed a very similar growth mode for Fe/Ti [30], Fe/Zr [31], and Co/Ti [32] bilayers.

Depending on the initial thickness  $d_i$  of the iron films, oxidation proceeds with a considerably different evolution in time. For samples with an initial thickness  $d_i = 10$  nm oxidation is accomplished within one day and is stopped after about 2.5 nm of metal has been transformed into oxide. We have not observed any degradation of the saturation magnetization of that sample after several months. Apparently this sample has acquired a stable oxide top layer. However, for an initial Fe thickness of less than about 5 nm the same oxidation process is considerably prolonged and requires now weeks or months until its completion.

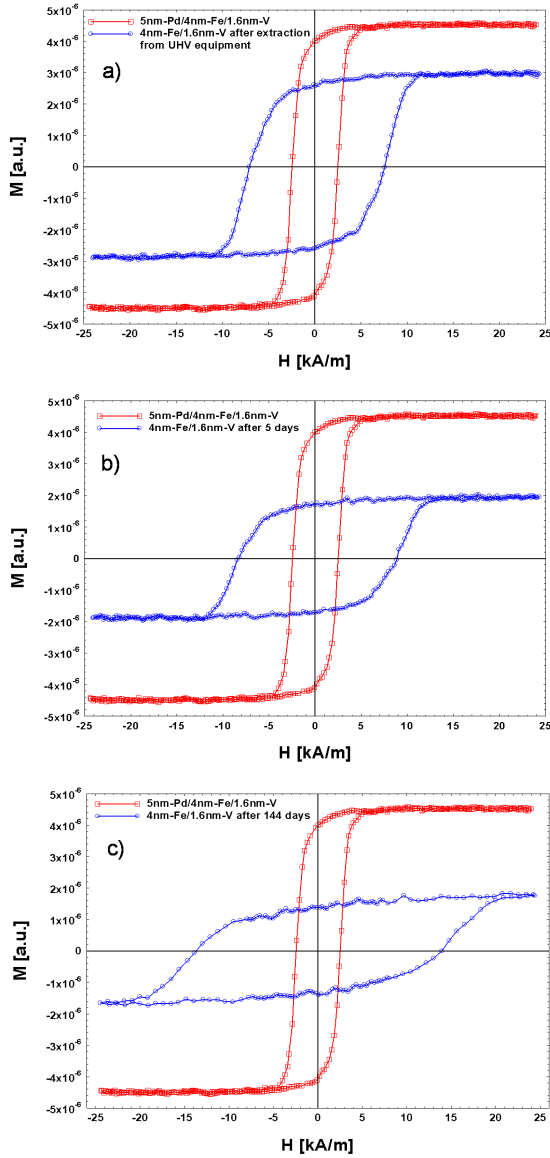


Fig. 2. Hysteresis loops (circles, blue lines) for Fe films with  $d_i = 4$  nm measured after extraction from UHV equipment (a), and after 5 (b) and 144 days (c) of exposure to ambient conditions. Hysteresis loops denoted by squares (red lines) were also measured at the same time for reference sample with  $d_i = 4$  nm covered against oxidation by a 5 nm Pd protection layer. The degradation of saturation magnetization of the non-protected sample (circles, blue lines) is due to the transformation of metallic Fe into an iron oxide. Measurements were performed at room temperature.

In Fig. 2 we give an example of how this can be evidenced with magnetization measurements. Here hysteresis curves are seen, taken on the same sample with an initial iron thickness of 4 nm immediately after an exposure to ambient condition (Fig. 2a, circles, blue line), after 5 (Fig. 2b, circles, blue line) and 144 (Fig. 2c, circles, blue line) days of exposure to ambient conditions. Hysteresis loops denoted by squares (red lines) are measured for reference sample with  $d_{\text{Fe}} = 4$  nm covered against oxidation

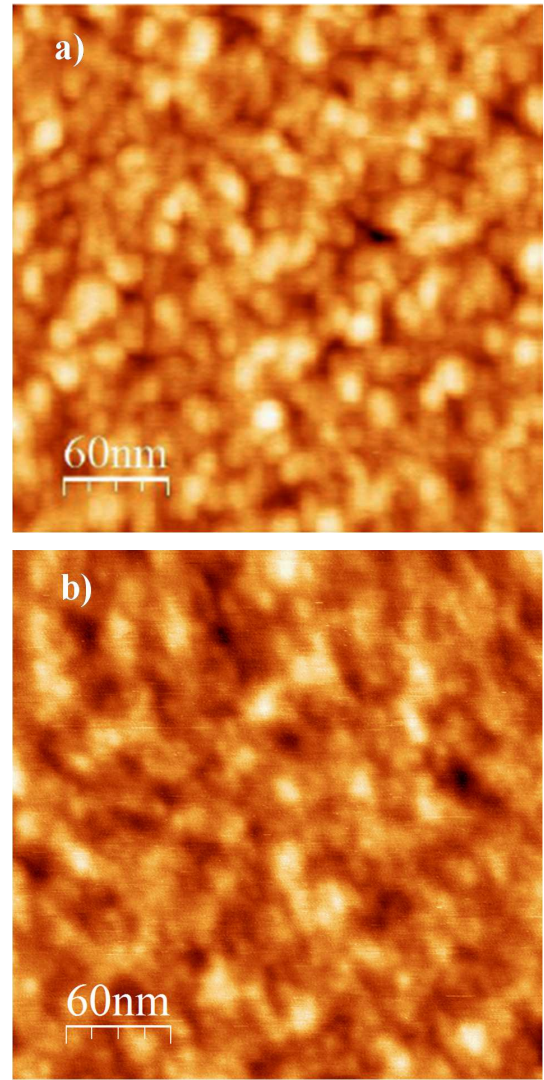


Fig. 3. AFM images measured for the Fe film with  $d_i = 4$  nm after 5 (a) and 144 days (b) of oxidation under ambient conditions.

by a 5 nm Pd protection layer. The degradation of saturation magnetization of the non-protected sample is due to the transformation of metallic Fe into iron oxides. The more interesting observation is the decreasing saturation magnetization with time due to a continuing oxidation. With increasing oxide layer thickness (decreasing hysteresis signal) the hysteresis curve gets gradually broader, as can be seen in Fig. 2.

It is well known, that the vanadium atoms near V–Fe interface polarise antiparallel to the iron atoms, especially at low temperatures [7, 33]. However, there are no reports on such a polarisation near interface between iron and its oxides. On the other hand, near Fe–Pd interface palladium atoms polarise parallel to the iron atoms, similarly to the effect observed earlier for Ni–Pd [34, 35] and Co–Pd [36] interfaces. As a result, for the reference sample compensate small negative and positive polarisations of V and Pd atoms, respectively.

In Fig. 3 we show AFM images obtained for the 4 nm-Fe/1.6 nm-V bilayer after 5 (a) and 144 days (b) of oxidation under ambient conditions. The images show actual morphology of the oxidised Fe top layer. The roughness measured for  $2 \mu\text{m} \times 2 \mu\text{m}$  area (not shown here) was about 0.20 nm and 0.21 nm for the sample after 5 and 144 days of oxidation, respectively. The relatively low values of the roughness parameters revealed planar growth of the oxidised layer.

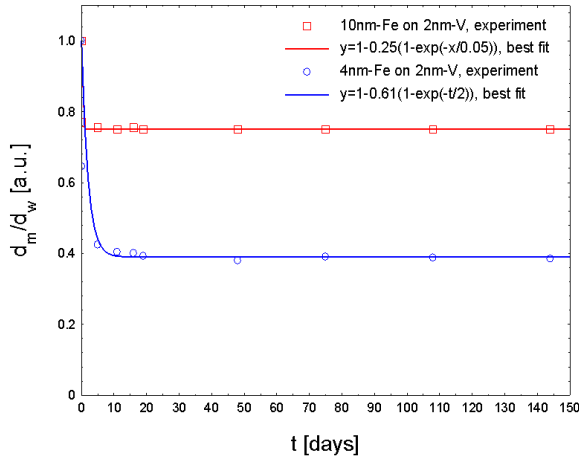


Fig. 4. Thicknesses of the ferromagnetic Fe layer  $d_m$  (from VSM measurements) relative to thicknesses of reference samples (protected against oxidations) as a function of time. Solid lines are exponentials using a time constant of oxidation of about 0.05 and 2 days for the initial Fe thickness equal to 10 and 4 nm, respectively.

Assuming bulk magnetisation of the metallic iron rest it was possible to illustrate the time evolution of the oxidation process by giving the magnetically evaluated Fe thickness  $d_m$ , as a function of time (see Fig. 4). For a quantitative description of this process we apply the same exponential law as for naturally oxidised Co films [4]:

$$d_m(t) = d_i - 2.5(1 - e^{-t/\tau}). \quad (1)$$

Equation (1) contains only the time constant  $\tau$  as a fit parameter and the solid line in Fig. 4 gives the best fits which result in a satisfactory description of the experimental features. The time constant was estimated as 0.05 and 2 days for  $d_i$  equal to 10 and 4 nm, respectively.

Thickness dependence of the time constant  $\tau$  was reported earlier for the polycrystalline and smooth cobalt thin films [4]. It was reported in Ref. [4] that for  $d_i < 5$  nm the time constant for oxidation increases considerably reaching an extrapolated value of  $\tau = 190$  days for  $d_i \rightarrow 0$ . On the other side, cobalt films with an initial thickness of  $d_i > 5$  nm oxidise instantaneously, whereby a constant amount of 2.5 nm of metal is transformed into oxide. As could be observed in Fig. 4, approximately the same amount of metallic iron (2.5 nm) was transformed to iron oxide.

In general, smooth iron thin films may exhibit different chemical properties responsible for oxidation com-

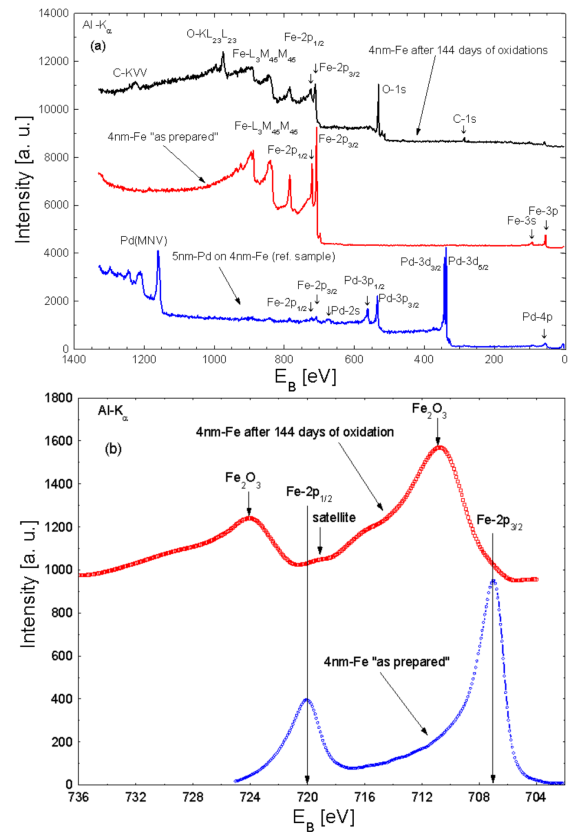


Fig. 5. XPS ( $\text{Al } K_{\alpha}$ ) spectra (a) of “as prepared” Fe thin film with an initial Fe thickness  $d_i = 4$  nm, measured *in situ* immediately after preparation and after 144 days of oxidation. For a comparison we also show XPS spectrum of 4 nm-Fe thin film covered by 5 nm-Pd protection layer (reference sample). XPS ( $\text{Al } K_{\alpha}$ ) spectra near Fe  $2p$  peaks (b) for “as prepared” 4 nm-Fe thin film and after 144 days of oxidation under atmospheric conditions were shown in part (b). Vertical arrows show positions of the Fe  $2p_{1/2}$  and Fe  $2p_{3/2}$  peaks for 4 nm Fe thin film measured *in situ* immediately after preparation and after 144 days of oxidation.

pared to those reported for cobalt. Our recent studies on iron growth on vanadium underlayer revealed the planar growth up to a thickness of about 5 nm [7]. For the greater thickness we have observed a transition to islands growth mode [7]. Therefore, we conclude that thinner Fe layers are more oxidation resistant than the thicker ones due to observed transition in the growth mode. The increasing time constant for oxidation let all iron ultra-thin films with  $d_i < 2.5$  nm appear ferromagnetic for a long time due to a nonoxidised metallic rest. Work on thickness dependence of oxidation of ultra-thin Fe films is in progress and results will be published in a separate paper.

The “as prepared” and oxidised thin Fe films were also characterised using XPS. Figure 5a shows XPS spectra of “as prepared” Fe thin film with an initial thickness  $d_i = 4$  nm, measured *in situ* immediately after preparation, and after 144 days of oxidation. For a comparison

we also show XPS spectrum of 4 nm-Fe thin film covered by 5 nm-Pd protection layer. The later thin film serves as the reference sample in magnetic measurements. Additionally, the XPS measurements were also carried out near the Fe  $2p$  peaks for the “as prepared” Fe thin film sample with  $d_i = 4$  nm and after 144 days of oxidation under ambient conditions. The corresponding XPS peaks of the Fe  $2p_{3/2}$  and Fe  $2p_{1/2}$  are shown in Fig. 5b. In the case of the “as prepared” thin film the Fe  $2p_{3/2}$  peak is narrower and stronger than Fe  $2p_{1/2}$  and the area of Fe  $2p_{3/2}$  peak is greater than that of Fe  $2p_{1/2}$ . The positions of the Fe  $2p$  peaks for the oxidised sample are considerably shifted and revealed formation of the Fe<sub>2</sub>O<sub>3</sub> (hematite) layer on the metallic iron rest. Formation of hematite thin film after 144 days of oxidation is also confirmed by observation of a weak satellite peak in the XPS spectrum for the oxidised sample (see Fig. 5b). Furthermore, the Fe  $2p_{3/2}$  and Fe  $2p_{1/2}$  peaks are broadened compared to those observed for the metallic iron thin film.

#### 4. Conclusions

Results of our studies show that for iron thin film with an initial thickness  $d_i = 10$  nm, oxidation is accomplished within one day, whereby a constant amount of 2.5 nm of metal is transformed into oxides. For Fe thickness lower than about 5 nm the time constant for oxidation increases reaching a value of 2 days for the initial Fe thickness equal to 4 nm. The XPS measurements after 144 days of natural oxidation of the 4 nm-Fe thin film revealed formation of Fe<sub>2</sub>O<sub>3</sub> (hematite) layer on metallic iron rest. The surprising observation that thinner Fe thin films are more oxidation resistant than the thicker ones could be associated with recently observed transition from planar to island growth mode for  $d_{Fe} \approx 5$  nm.

#### Acknowledgments

MN and RC acknowledge the support from The Ministry of Science and Higher Education (Project No. 06/62/DSPB/2172).

#### References

- [1] T. Fujii, F.M.F. de Groot, G. Sawatzky, F.C. Voogt, T. Hibma, K. Okada, *Phys. Rev. B* **59**, 3195 (1999).
- [2] R. Cornell, U. Schwertmann, *The Iron Oxides*, Wiley, New York 1997.
- [3] M. Monti, B. Santos, A. Mascaraque, O. Rodriguez de la Fuente, M.A. Niño, T.O. Mentês, A. Locatelli, K.F. McCarty, J.F. Marco, J. de la Figuera, *J. Phys. Chem. C* **116**, 11539 (2012).
- [4] L. Smardz, U. Köbler, W. Zinn, *J. Appl. Phys.* **71**, 5199 (1992).
- [5] L. Smardz, U. Köbler, W. Zinn, *Vacuum* **42**, 283 (1991).
- [6] J.D. Baran, H. Grönbeck, A. Hellman, *Phys. Rev. Lett.* **112**, 146103 (2014).
- [7] A. Marczyńska, J. Skoryna, B. Szymanski, L. Smardz, *Acta Phys. Pol. A* **127**, 552 (2015).
- [8] D. Briggs, M.P. Seah, *Practical Surface Analysis*, Wiley, New York 1990.
- [9] S.J. Roosendaal, B. van Asselen, J.W. Elsenaar, A.M. Vredenberg, F.H.P.M. Habraken, *Surf. Sci.* **442**, 329 (1999).
- [10] P.C.J. Graat, M.A.J. Somers, *Appl. Surf. Sci.* **100–101**, 36 (1996).
- [11] P.C.J. Graat, M.A.J. Somers, *Surf. Interface Anal.* **26**, 773 (1998).
- [12] C. Ruby, B. Humbert, J. Fusy, *Surf. Interface Anal.* **29**, 377 (2000).
- [13] A. Mekki, D. Holland, C.F. McConville, M. Salim, *J. Non-Cryst. Solids* **208**, 267 (1996).
- [14] T. Yamashita, P. Hayes, *J. Electron Spectrosc. Relat. Phenom.* **152**, 6 (2006).
- [15] T. Yamashita, P. Hayes, *Appl. Surf. Sci.* **254**, 2441 (2008).
- [16] L. Smardz, K. Le Dang, H. Niedoba, K. Chrzumnicka, *J. Magn. Magn. Mater.* **140–144**, 569 (1995).
- [17] L. Smardz, *Solid State Commun.* **112**, 693 (1999).
- [18] L. Smardz, *J. Alloys Comp.* **395**, 17 (2005).
- [19] L. Smardz, K. Smardz, H. Niedoba, *J. Magn. Magn. Mater.* **220**, 175 (2000).
- [20] J. Skoryna, A. Marczyńska, M. Lewandowski, L. Smardz, *J. Alloys Comp.* **645**, 280 (2015).
- [21] A. Marczyńska, J. Skoryna, L. Smardz, *Acta Phys. Pol. A* **126**, 1315 (2014).
- [22] L. Smardz, *J. Magn. Magn. Mater.* **240**, 273 (2002).
- [23] L. Smardz, M. Jurczyk, K. Smardz, M. Nowak, *Czechoslov. J. Phys.* **52**, A177 (2002).
- [24] L. Smardz, M. Nowak, M. Jurczyk, *Int. J. Hydrogen Energy* **37**, 3659 (2012).
- [25] L. Smardz, M. Jurczyk, K. Smardz, M. Nowak, M. Makowiecka, I. Okońska, *Renew. Energy* **33**, 201 (2008).
- [26] K. Smardz, L. Smardz, I. Okonska, M. Nowak, M. Jurczyk, *Int. J. Hydrogen Energy* **33**, 387 (2008).
- [27] M. Jurczyk, L. Smardz, M. Makowiecka, E. Jankowska, K. Smardz, *J. Phys. Chem. Solids* **65**, 545 (2004).
- [28] J. Skoryna, A. Marczyńska, L. Smardz, *J. Alloys Comp.* **645**, S384 (2015).
- [29] J. Skoryna, S. Pacanowski, A. Marczyńska, M. Werwiński, Ł. Majchrzycki, R. Czajka, L. Smardz, *Surf. Coat. Technol.* **303**, 125 (2016).
- [30] L. Smardz, K. Smardz, *Mater. Sci.-Poland* **24**, 821 (2006).
- [31] K. Smardz, L. Smardz, *Phys. Status Solidi B* **243**, 227 (2006).
- [32] L. Smardz, K. Smardz, R. Czajka, *Cryst. Res. Technol.* **36**, 1019 (2001).
- [33] J. Skoryna, M. Wachowiak, A. Marczyńska, A. Rogowska, Ł. Majchrzycki, W. Koczorowski, R. Czajka, L. Smardz, *Surf. Coat. Technol.* **303**, 119 (2016).
- [34] L. Smardz, *J. Magn. Magn. Mater.* **83**, 119 (1990).
- [35] L. Smardz, B. Szymanski, J. Barnaś, J. Baszyński, *J. Magn. Magn. Mater.* **104–107**, 1885 (1992).
- [36] L. Smardz, J. Baszyński, B. Rauschenbach, *Thin Solid Films* **175**, 2915 (1989).